

# Active circle swimmers as hyperuniform systems

workshop on *Hyperuniform structures, rigid point processes and related topics*

Lille (France)



20.-22.02.2023



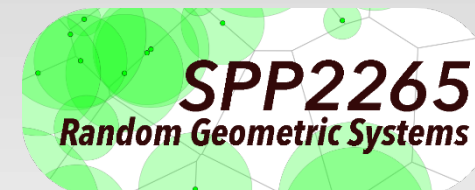
<https://www.fotocommunity.de/photo/duesseldorf-rheinturm-und-neuer-zollho-andreas-1957/30660517>

Hartmut Löwen

Heinrich-Heine-Universität  
Düsseldorf



- 1) Introduction to circle swimming
- 2) Interacting circle swimmers
- 3) Hyperuniformity in active systems
- 4) Conclusions



# 1) Introduction to circle swimming

Circle swimming of Phalarope birds



<https://www.youtube.com/watch?v=heEUPbxmYgQ>

## Kinematics of phalarope spinning

SIR — Phalaropes are wading birds that spin on the water, presumably to feed<sup>1–5</sup> because they peck while spinning. Recently, we demonstrated with high-speed photography that phalaropes do indeed feed while spinning<sup>6</sup>. These very small birds are the only vertebrates that spin. Larger birds probably could not spin fast enough to upwell prey. Spinning is energetically costly, about four times resting metabolism — phalaropes do not spin if adequate surface prey are available. Here we report the details of how these birds feed while spinning.

We first thought that phalaropes produce a bounded vortex with central

between 35° and 50°. The bird leans in and circles with a radius of half the waterline length, the bill above the upwelled core. The bird's body circles continuously, but its head moves in discrete 45° snaps, separated by brief pauses, like a spinning ballerina. Phalaropes detect prey, thrust, seize, transport and swallow in less than half a second<sup>6</sup>, at a rate of 180 pecks per minute<sup>7</sup>.

We simulated water circulation generated by spinning phalaropes with a motorized toy submarine attached rigidly to a surface float, with the propeller at the same depth as the feet of the bird. The 10-cm submarine generated a rotational eddy in solid-body rotation within the turning circle and an irrotational eddy outside, identical to that produced by phalaropes<sup>8</sup>. Upwelling began nearly instantaneously in the centre of the circle. The water surface bounded the upwelled water, which was deflected radially in a 2-cm layer. The flow was thus strongly three-dimensional, with comparable vertical and radial velocities and an upwelling depth of ten times the radius.

Phalaropes kick water away at the surface so rapidly that the water surface is depressed and deeper water flows upwards to replace it. The bird thus deflects the free surface, driving an upward momentum jet. This intense upwelling differs from classical oceanographic upwelling, wherein vertical velocity is smaller than horizontal velocity by several orders of magnitude. When phalaropes spin they swim sideways (Fig. 2), moving their centre of rotation and extracting food from new areas.

In 1.5-m-deep aquaria, particles 0.5 m under the submarine were upwelled, but in those shallower than 0.5 m a boundary layer developed on the bottom<sup>9</sup>, with central upwelling. When spinning ceased, the bottom was cleared under the turning circle. This also occurred when phalaropes spun over a dish with dead brine shrimp immersed in brine stained with dye. A green, tornado-like tube of dye and prey rose upward from the dish (Fig. 1), rotating opposite to the rotation of the bird as it began to feed.

Spinning concentrates prey into the upwelling jet where the phalarope feeds faster than any other bird. Rapid, localized feeding is effective when food is patchy or out of reach, as with the bird's planktonic prey at sea. Spinning is effective when prey are aggregated and layered against a shallow bottom and subject to accumulation by medially directed bottom currents and when prey are layered or immobilized by cold<sup>10</sup>. Tinbergen noted<sup>2</sup> that phalaropes do not spin when it is windy. Wind-

Photograph by B. Uebelhake

IMAGE  
UNAVAILABLE  
FOR COPYRIGHT  
REASONS

circle  
swimming

FIG. 1 Spinning red-necked phalarope generates an upwelled plume of prey (brine shrimp) and fluorescein dye. Birds were induced to feed in a 1-m<sup>2</sup> aquarium by placing brine shrimp in an open petri dish on the bottom, in water shallow enough for the birds to reach the food by dipping the bill and head under water. The water level was then raised gradually until the birds spontaneously spun to feed. Flow patterns were revealed by filling the petri dish with hypersaline water mixed with fluorescein dye and prey that remained in the dish until the birds began to spin.

upwelling, but Sutton<sup>1</sup> and others<sup>4</sup> report phalaropes "twirling in water many fathoms deep", far too deep for toroidal flow. Instead, red-necked phalaropes produce a subsurface meridional flow that concentrates and upwells prey in an upward momentum jet due to differential effort by the legs (Fig. 1). Each 1-second spin requires 7–8 kicks. The lobed toes spread for thrust and fold for recovery. The outer tarsus travels through an angle between 90° and 110°, the inner only

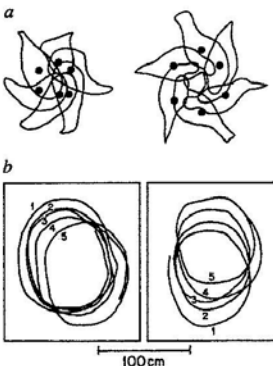


FIG. 2 Motion analysis of a spinning phalarope. Phalaropes in the aquarium were videotaped from above and feeding was analysed in two dimensions using an ExpertVision motion analysis system (Motion Analysis Corp., Santa Rosa, California). *a*, Outline of a phalarope during a single spin in a digitized sequence. Filled circles, centroids of the bird's outline in each video frame. *b*, Frame-by-frame centroid tracks for two birds during five sequential spins. Each spin was slightly offset from the former so that the spinning phalarope travelled slowly over the water; spinning velocity for five sequences with three different birds averaged  $0.28 \text{ m s}^{-1}$  ( $\text{s.d.} = 0.03 \text{ m s}^{-1}$ ).

generated surface shear, Langmuir cells, and breaking waves may interfere with bird-generated upwelling jets.

**Bryan S. Obst\***

**William M. Hamner**

**Peggy P. Hamner**

*Department of Biology,  
University of California, Los Angeles,  
California 90095-1606, USA*

**Eric Wolanski**

*Australian Institute of Marine Science,  
P. M. B. no. 3, MSO, Townsville,  
Queensland 4810, Australia*

**Margaret Rubega**

*Department of Environmental and  
Resource Sciences,  
University of Nevada at Reno,  
Reno, Nevada 89512, USA*

**Bates Littlehales**

*25 Granite St, Ashland,  
Oregon 97520, USA*

1. Sutton, G. M. *Carnegie Mus.* **12**, 1–275 (1932).

2. Tinbergen, N. *Nature* **19**, 22 (1939).

3. Marshall, C. W. *Condor* **40**, 85 (1938).

4. Johns, J. E. *Auk* **86**, 660–670 (1969).

5. Hohn, E. O. *Ibis* **113**, 335–348 (1971).

6. Rubega, M. & Obst, B. S. *Auk* **110**, 169–178 and frontispiece (1993).

7. Mercier, F. M. & Gaskin, D. E. *Can. J. Zool.* **63**, 1062–1067 (1985).

8. Wolanski, E. *Physical Oceanographic Processes of the Great Barrier Reef* (CRC, Boca Raton, Florida, 1994).

9. Wolanski, E. et al. *J. Geophys. Res.* **89**, 10533–10569 (1984).

\*Deceased. Address correspondence to W. M. H.

Birds create  
hydrodynamic flow to  
float prey upwards

# Circling of human walkers

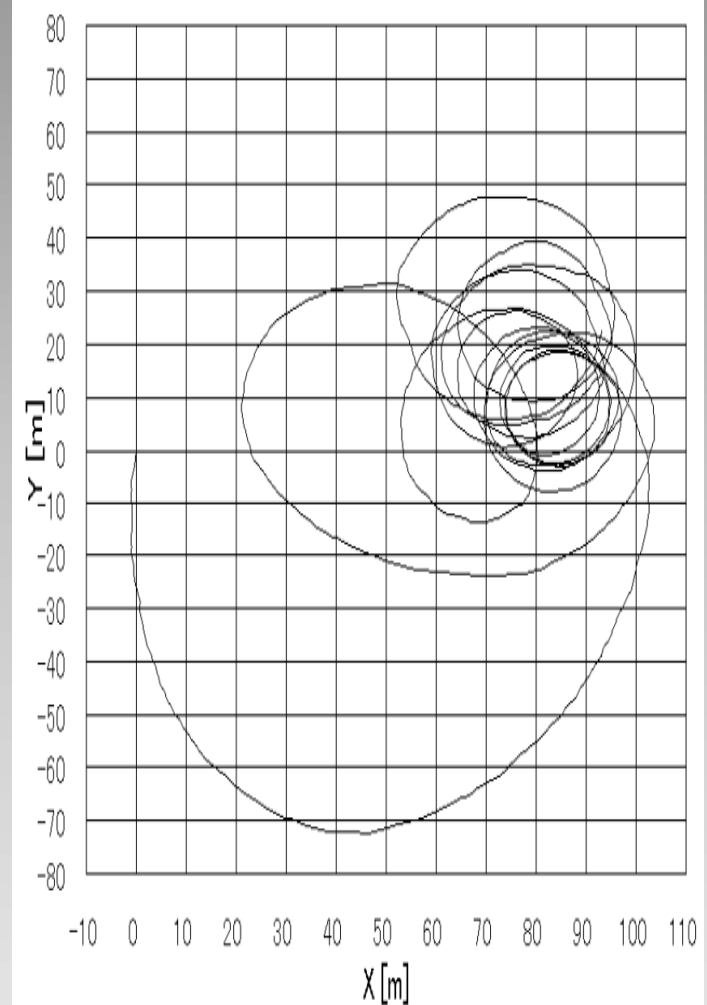


## ■ Trajectory of "Sample 5"

T. Obata et al., *J. Korean Phys. Soc.* **46**, 713 2005

But CAVEAT:

J.L. Souman et al, *Current Biology* **19**, 1538 (2009)



# Active Brownian motion of circle swimming

forces

$$\gamma \dot{\vec{r}}(t) = \gamma v_0 \hat{u}(t) + \vec{f}(t)$$

torques

$$\gamma R \dot{\phi}(t) = g(t) + M$$

external or internal torque

$$\hat{u}(t) = \begin{pmatrix} \cos \phi(t) \\ \sin \phi(t) \end{pmatrix}$$

$$\begin{aligned} \bar{\vec{f}}(t) &= 0 & \overline{f_i(t)f_j(t')} &= 2k_B T \gamma \delta(t - t') \delta_{ij} \\ \bar{g}(t) &= 0 & \overline{g(t)g(t')} &= 2k_B T \gamma_R \delta(t - t') \end{aligned}$$

(van Teffelen, HL, PRE 78, 020101 (2008))

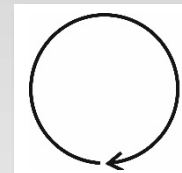
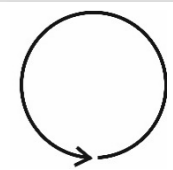
Gaussian noise

- $\phi(t)$  still Gaussian distributed (shifted Gaussian)
- no noise: trajectories are closed circles with radius and spinning frequency

$$\omega = \frac{M}{\gamma_r}$$

$$R = \frac{\gamma R v_0}{M}$$

- sign of M determines whether there is **clockwise** or **anti-clockwise** motion



# Brownian circle swimming: trajectories

$$F = \gamma v_0$$

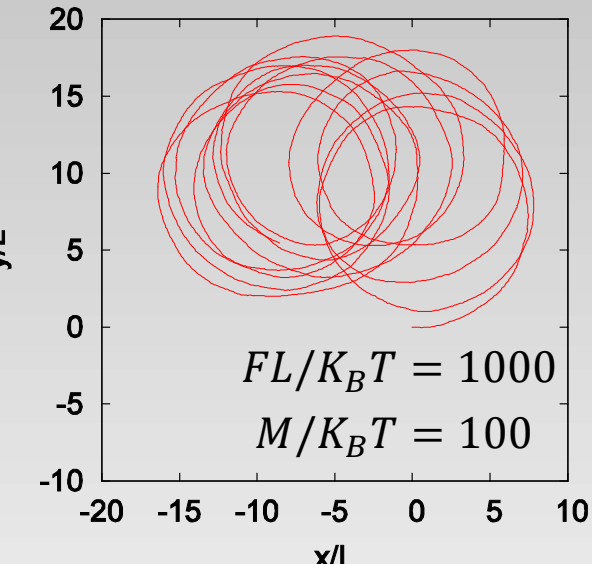
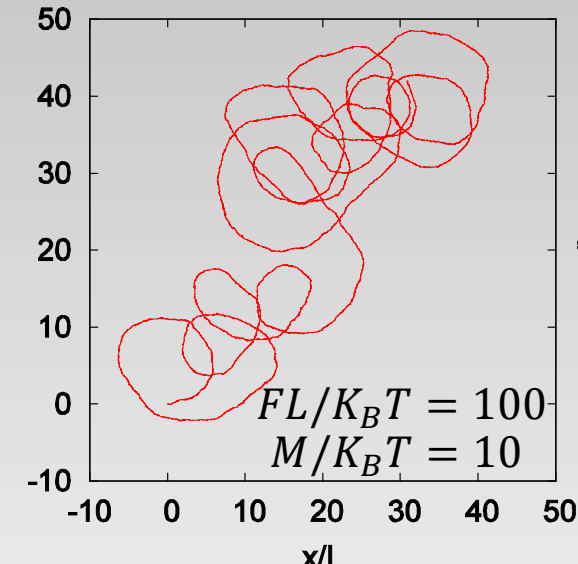
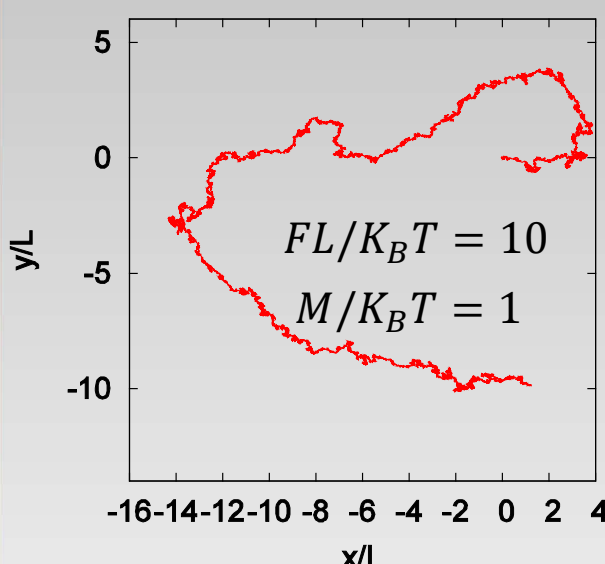
$L$  length unit

$$\tau_B = \frac{L^2}{D}$$



$$F = \frac{60K_B T}{L}, M = 8K_B T, t_{\max} = 2\tau_B$$

$$F = \frac{1000K_B T}{L}, M = 100K_B T, t_{\max} = 0,5\tau_B$$



# Mean displacement of circle swimmers

$$\overline{\vec{r}(t) - \vec{r}(0)} = \lambda [D_r \hat{u}_0 + \omega \hat{u}_0^\perp - e^{-D_r t} (D_r \bar{\hat{u}} + \omega \bar{\hat{u}}^\perp)] \quad (*) \quad \lambda = \frac{v_0}{D_r^2 + \omega^2}$$

$$\hat{u}_0^\perp = (-\sin \phi(0), \cos \phi(0)) \perp \hat{u}(0)$$

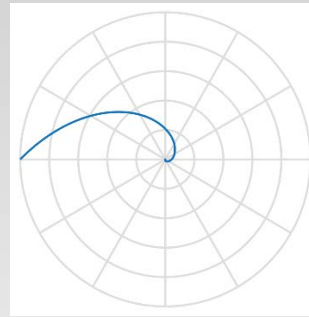
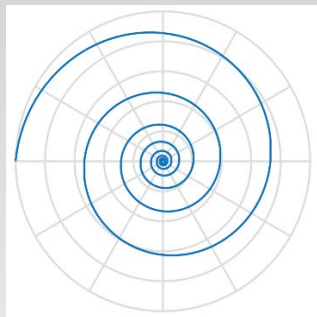
$$\bar{\phi}(t) = \phi_0 + \omega t \equiv \bar{\phi} \quad (**)$$

$$\bar{\hat{u}} = (\cos \bar{\phi}, \sin \bar{\phi}) \quad \bar{\hat{u}}^\perp = (-\sin \bar{\phi}, \cos \bar{\phi}) \perp \bar{\hat{u}}$$

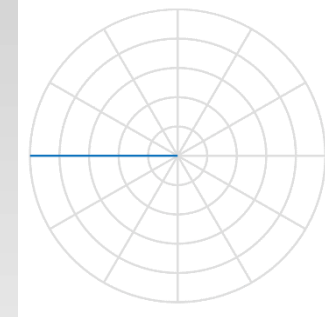
eliminate  $t$  in (\*),

spira mirabilis

$$\rightarrow r(\bar{\phi}) \sim \exp(-D_r(\bar{\phi} - \phi_0)/\omega)$$



M small

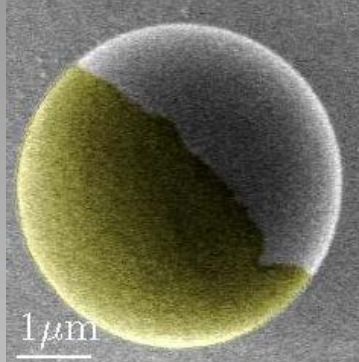


M = 0

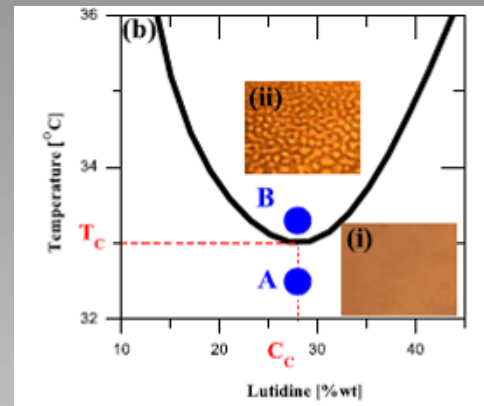


# Self-propulsion by demixing

Hertlein, Helden, Gambassi, Dietrich, Bechinger, Nature 451, 172 (2008)

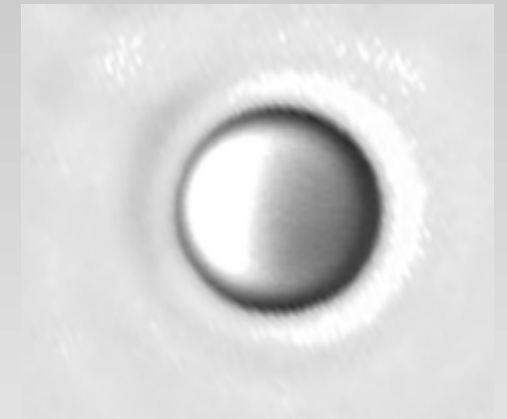
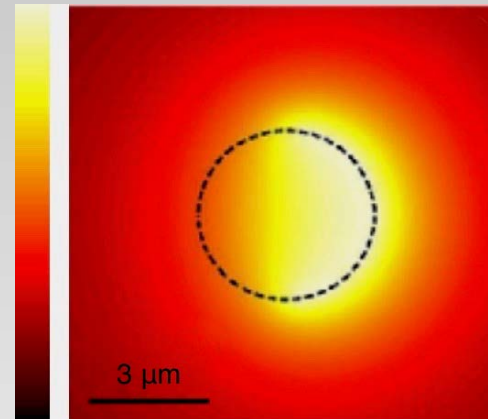
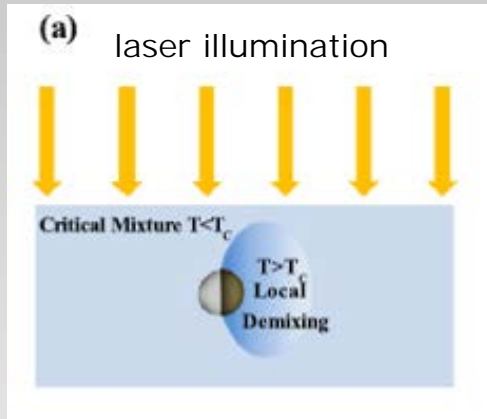


+



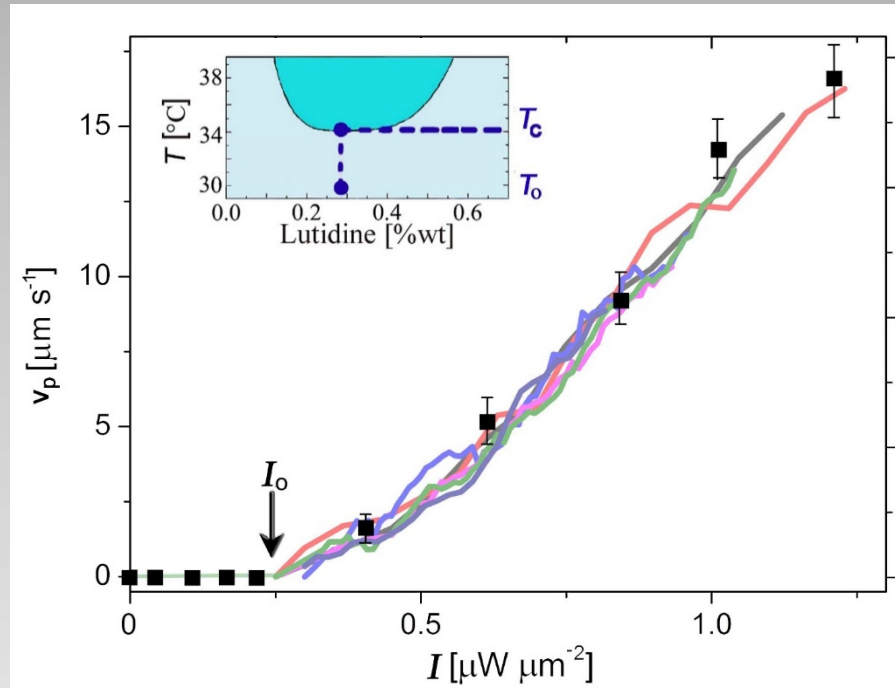
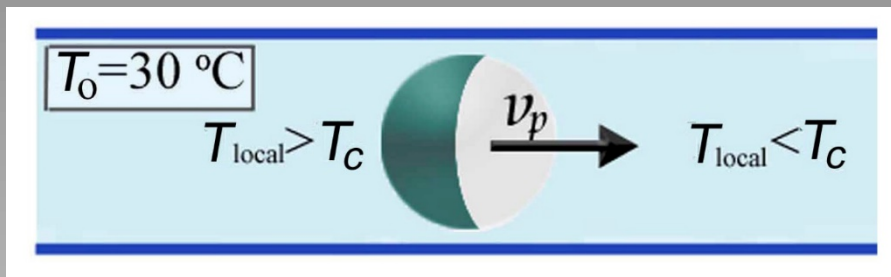
carbon-coated silica particles suspended in a binary mixture of water and lutidine

localized demixing of the mixture due to a heating of the cap



Volpe, Buttinoni, Vogt, Kümmerer, Bechinger, Soft Matter 7, 8810 (2011)

# Self-propulsion for small laser intensities



no laser illumination ( $I=0$ )  
→ no temperature gradient  
→ equilibrium  
→ no self-motion

for small intensities **linear relation**  
between illumination intensity and  
propulsion velocity beyond an  
intensity threshold  $I_0$

# Active colloidal particles

C. Bechinger, R. di Leonardo, H. Löwen, C. Reichhardt, G. Volpe, G. Volpe,

*Active particles in complex and crowded environments*

Reviews of Modern Physics **88**, 045006 (2016)



C. Bechinger



R. di Leonardo



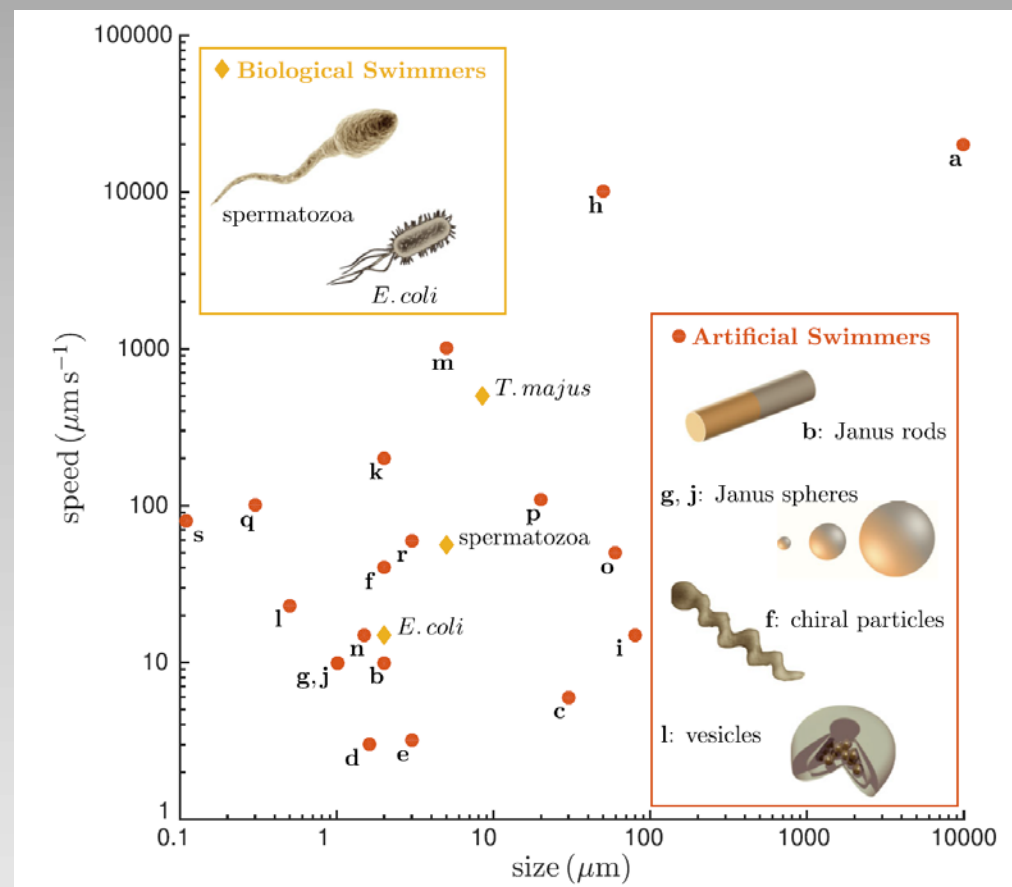
C. Reichhardt



G. Volpe

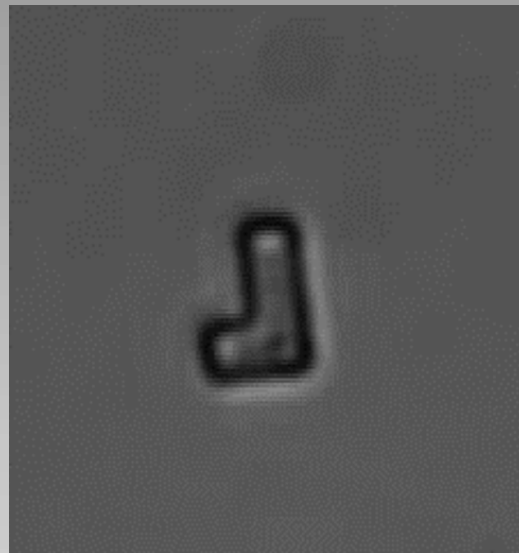
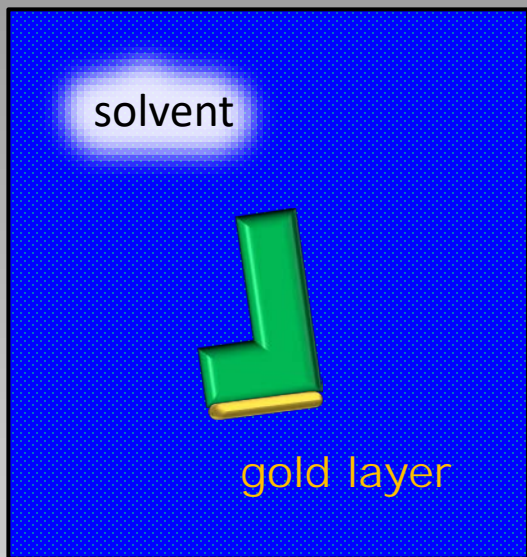


G. Volpe

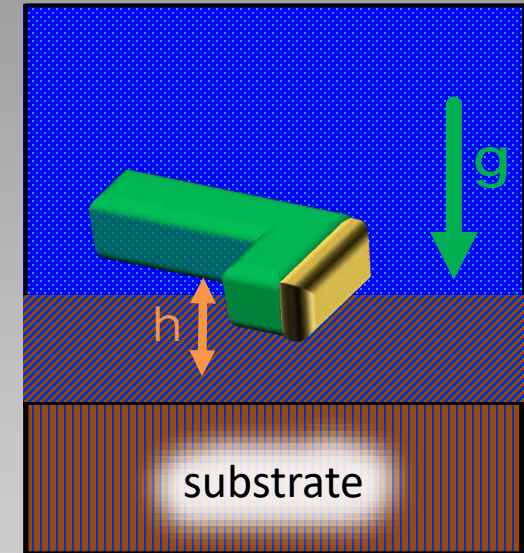


# Brownian circle swimmers (experiment)

top view



side view



asymmetric L-shaped particle  
motion on a substrate confined by gravity

What is the motion of the L-particle like?

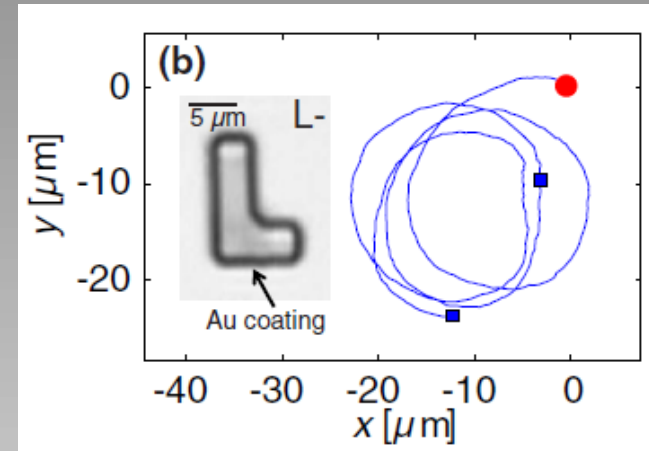
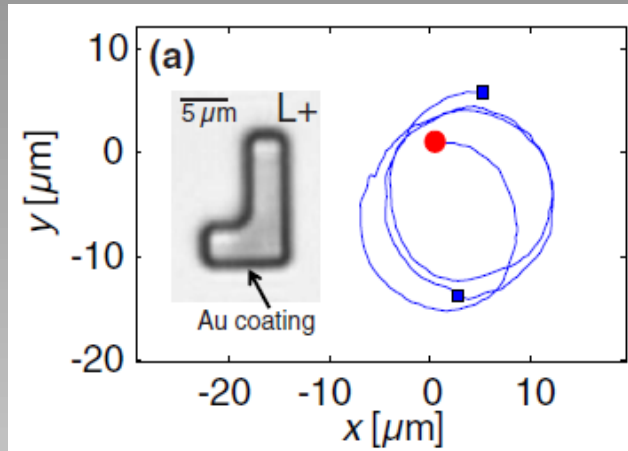
A no motion

B clockwise motion

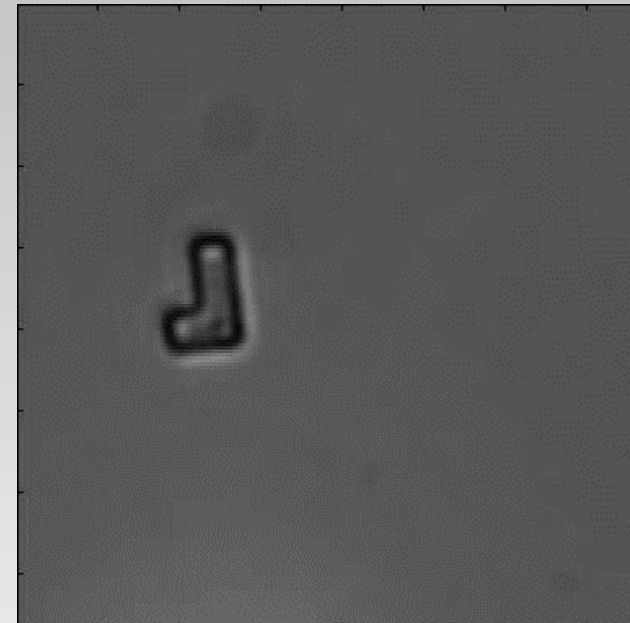
C anti-clockwise motion

D straight line

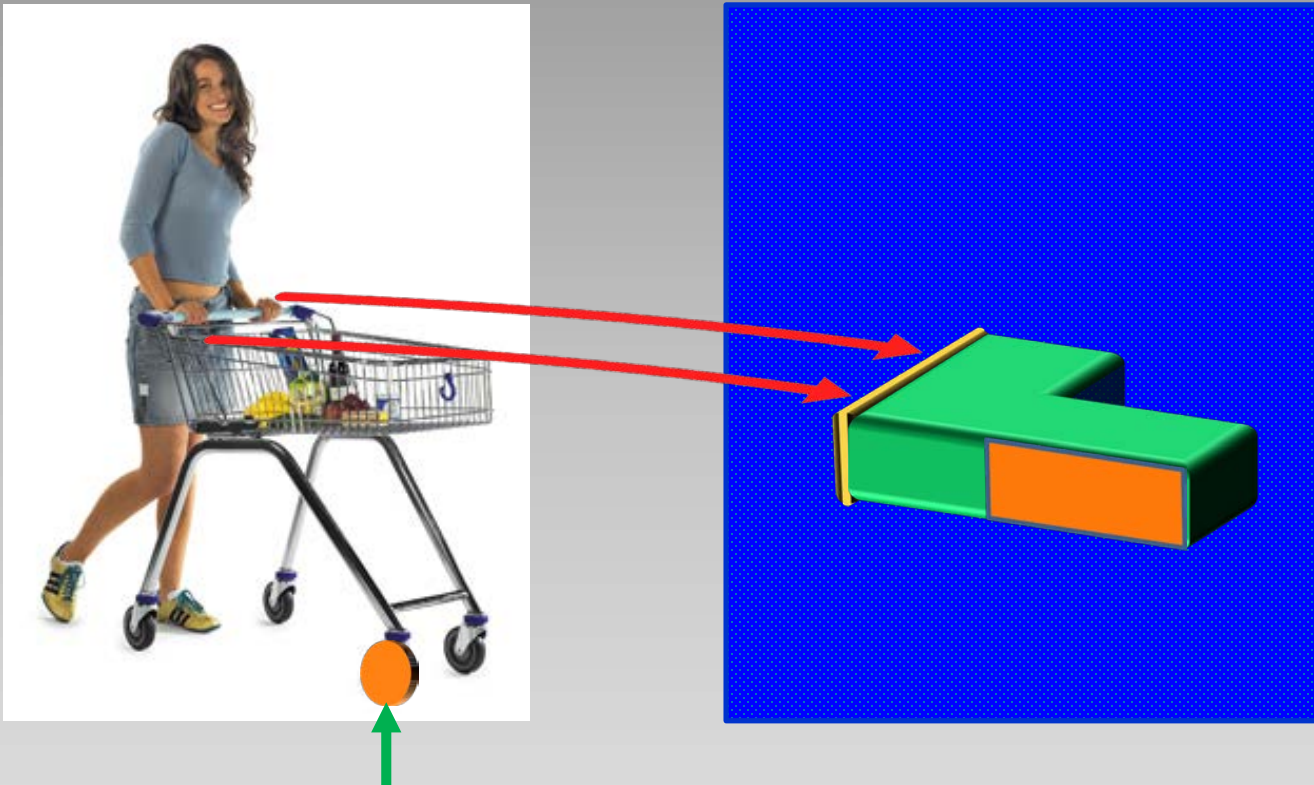
## chiral L-shaped particles



A pronounced circular motion is observed where the direction of rotation depends on the chirality of the particle.

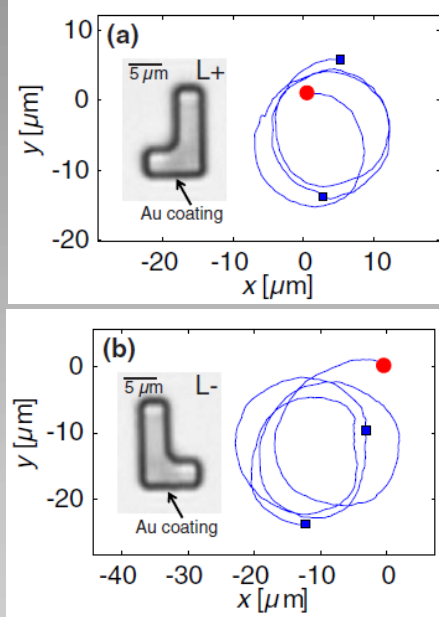


intuitive argument:  
pushing a shopping cart



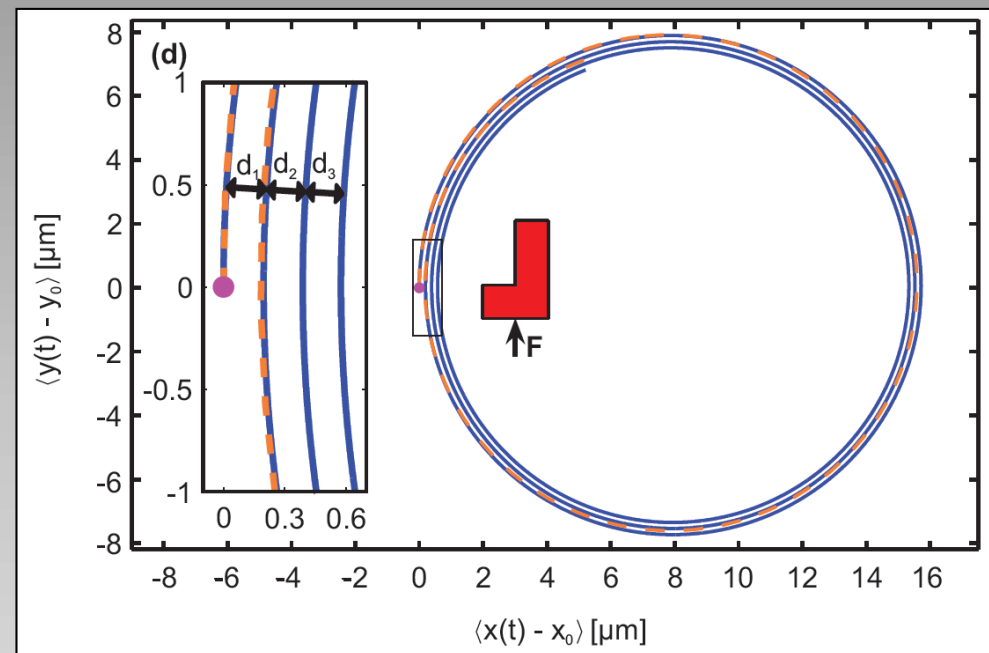
wheel with large friction

## chiral L-shaped particles



B. ten Hagen

F. Kümmel, B. ten Hagen, R. Wittkowski, I. Buttinoni, G. Volpe, H. Löwen, C. Bechinger, PRL **110**, 198302 (2013)



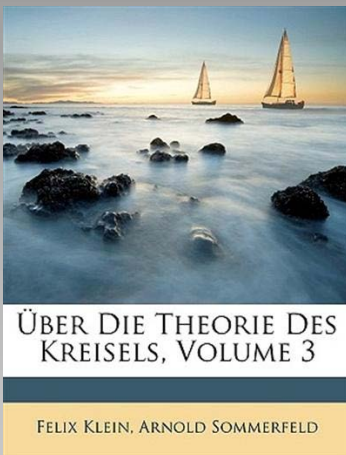
*spira mirabilis* for the noise-averaged trajectory

S. van Teeffelen, HL, Phys. Rev. E. 78, 020101 (2008)

# Brownian circle swimmers in 3d

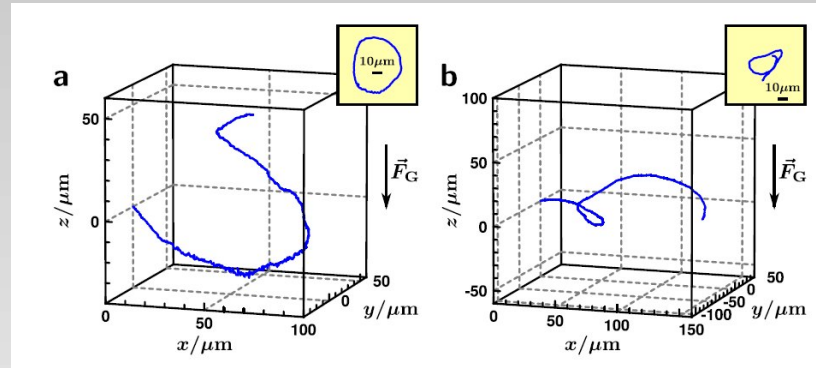
## Helical-like swimming in three dimensions: The Brownian spinning top

molecular dynamics



1897–1910

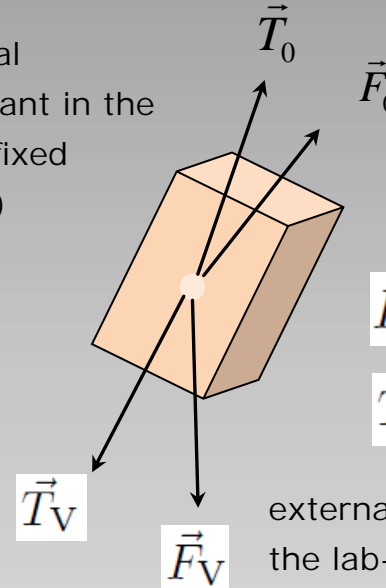
3d tracking of self-propelled colloids



A. Campbell, R. Wittkowski, B. ten Hagen, HL,  
S. J. Ebbens, JCP **147**, 084905 (2017)

self-propelled biaxial particle (in 3d)

internal  
(constant in the  
body-fixed  
frame)



$$\vec{F}_V = -\vec{\nabla}_{\vec{r}} U$$
$$\vec{T}_V = -\vec{\nabla}_{\vec{\omega}} U$$



R. Wittkowski

external (constant in  
the lab-frame)

- complicated equations of motion (see de la Torre et al, Doi for passive particles)
- translation-rotation coupling for a chiral particle (Brenner et al)

R. Wittkowski, HL, PRE **85**, 021406 (2012)

## 2) Interacting circle swimmers

equations of motion for many active Brownian circle swimmers (2d)

<i>forces</i>	$\gamma \dot{\vec{r}}_i(t) = -\nabla_i U + v_0 \hat{u}_i(t) + \vec{f}_i(t)$	<i>position</i>
<i>torques</i>	$\gamma R \dot{\varphi}_i(t) = g_i(t) + M$	<i>orientation</i>

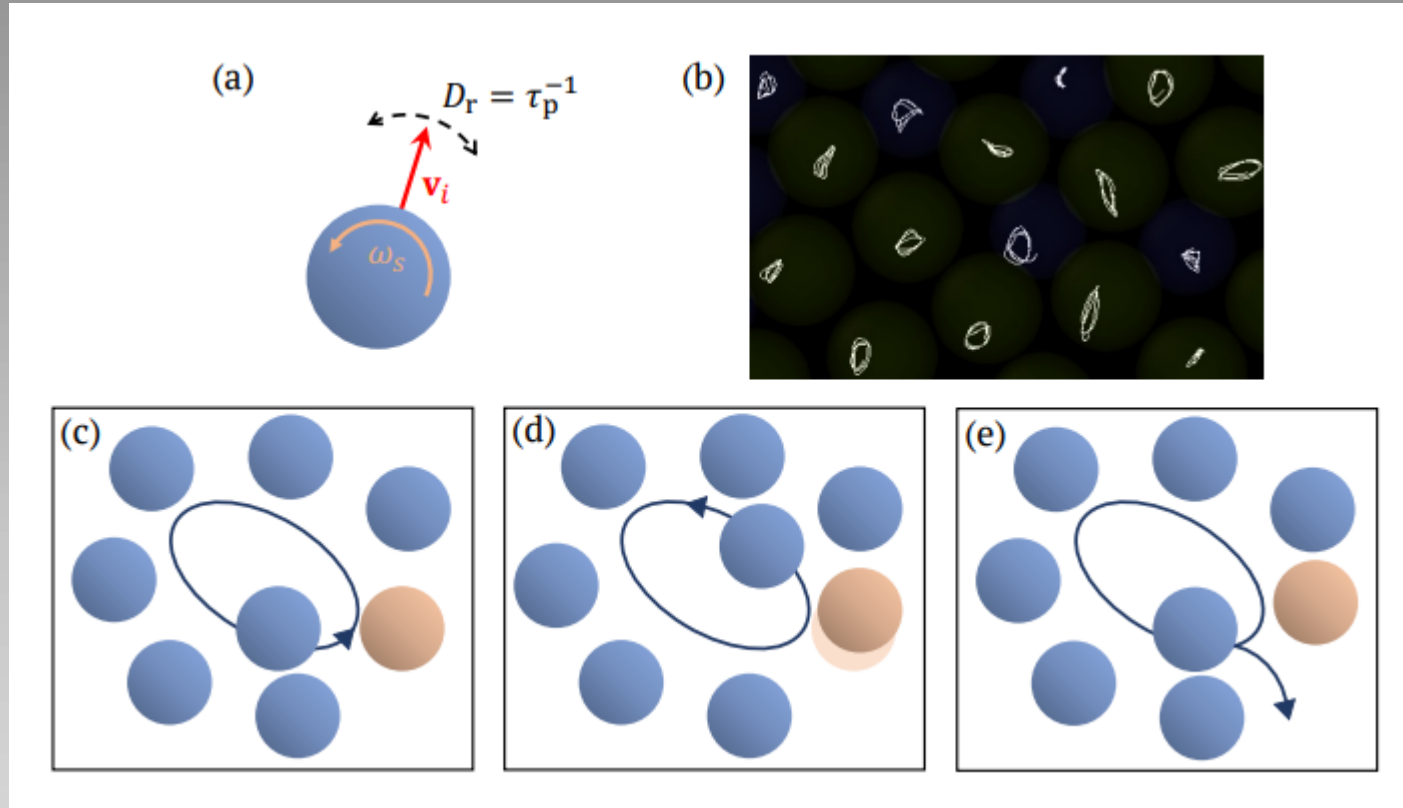
$$\hat{u}_i = \begin{pmatrix} \cos \varphi_i(t) \\ \sin \varphi_i(t) \end{pmatrix}$$

rotational noise decoupled, free rotational diffusion,  
no explicit aligning interactions as a minimal model

$$U = \sum_{j < i} u(|\mathbf{r}_i - \mathbf{r}_j|)$$

$u(r)$  WCA potential with soft core radius  $a$

# circle swimming in the cage of circle swimming neighbours



V. E. Debets, HL, L. M. C. Janssen,  
*Glassy Dynamics in Chiral Fluids,*  
Physical Review Letters **130**, 058201  
(2023)

V. Debets



L. Janssen



# glassy dynamics for dense circle swimmers

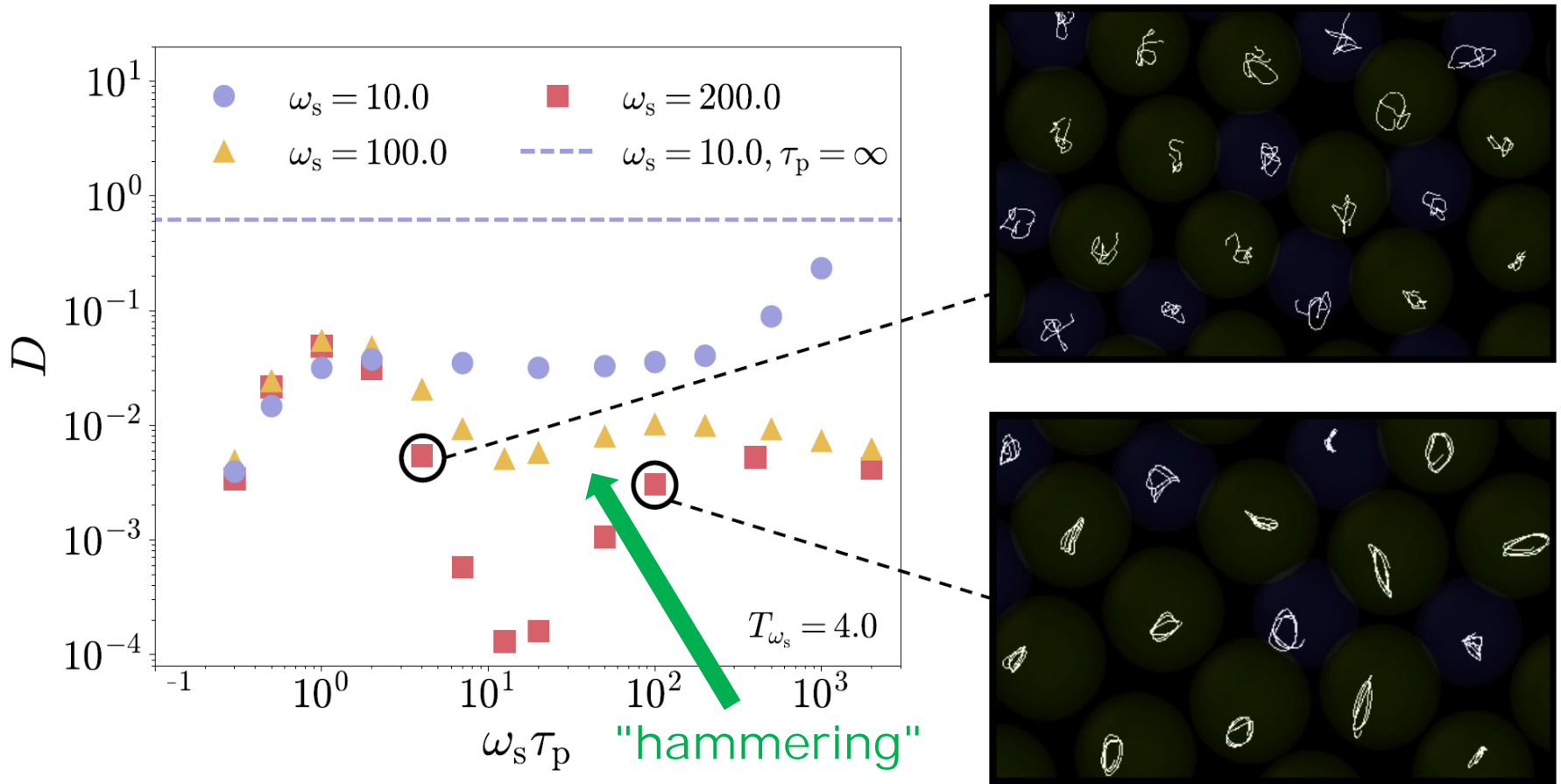
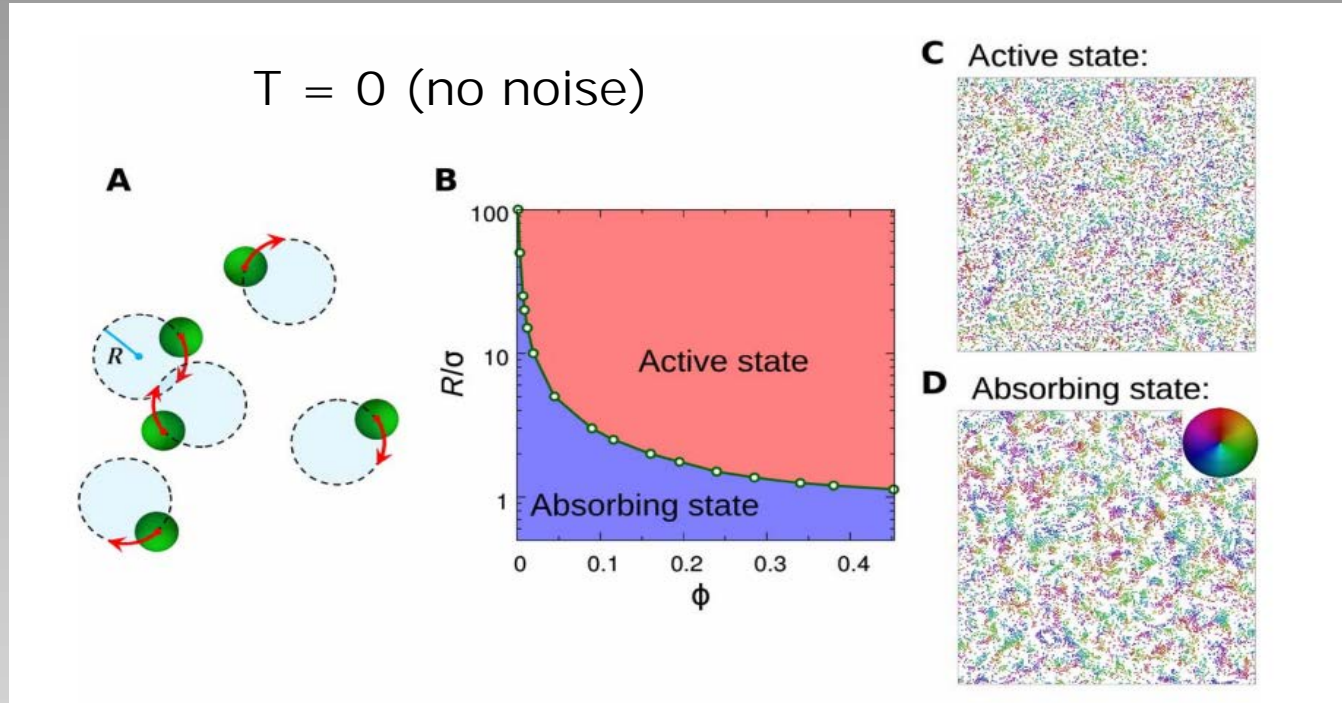
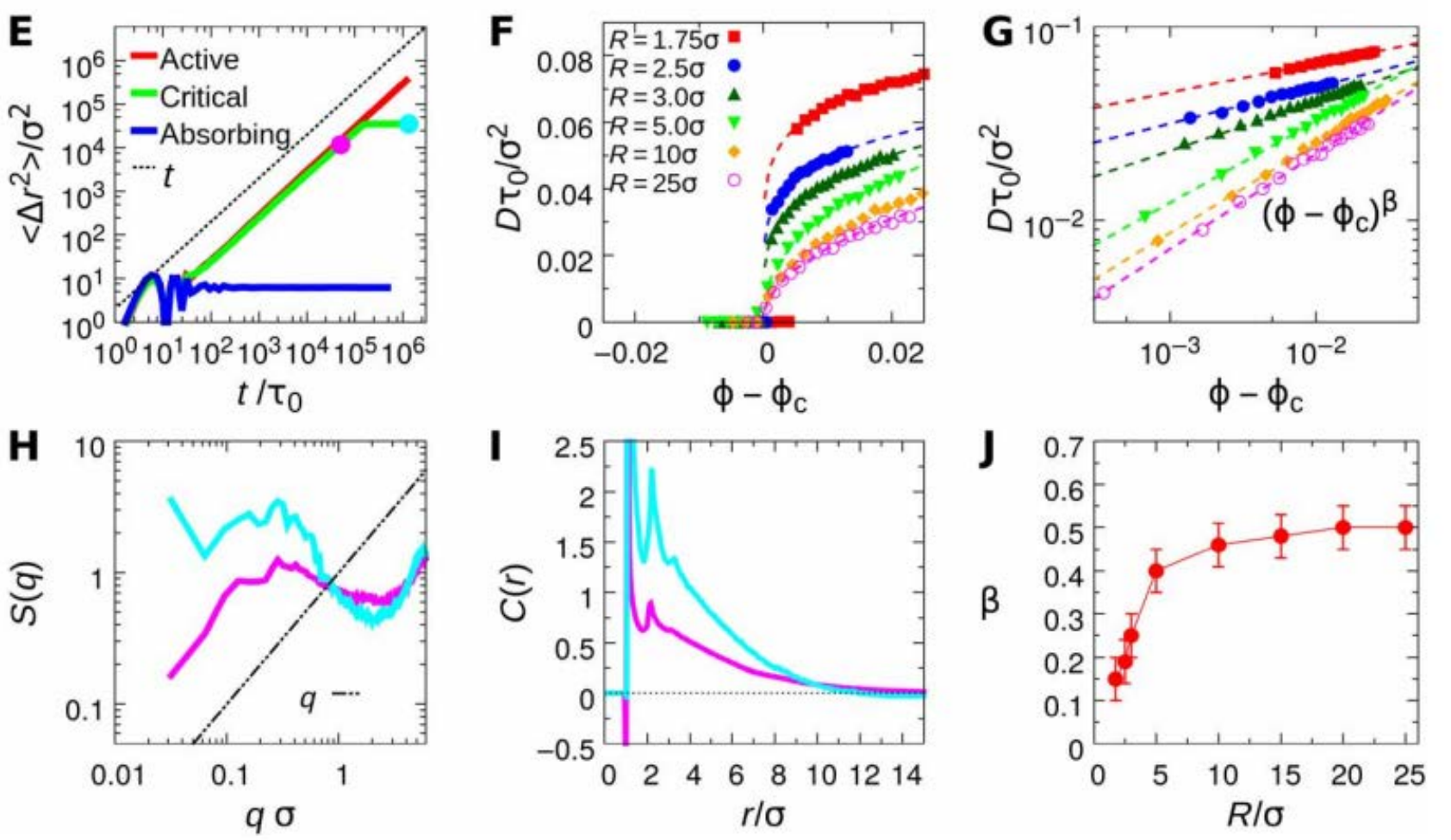


FIG. S7. Plot of the long-time diffusion coefficient  $D$  as a function of the normalized persistence time  $\omega_s \tau_p$ , which is also shown in the main text (Fig. 2). We highlight a number of short-time trajectories (total time is equal to three spinning periods  $3\tau_\omega$ ) for the two circled data points. It can be seen that for  $\omega_s \tau_p = 4.0$  (or  $\tau_p \sim \tau_\omega$ ) the trajectories show small signs of circular motion. In comparison, for  $\omega_s \tau_p = 100.0$  (or  $\tau_p \gg \tau_\omega$ ) the circular motion inside the cage becomes very pronounced.

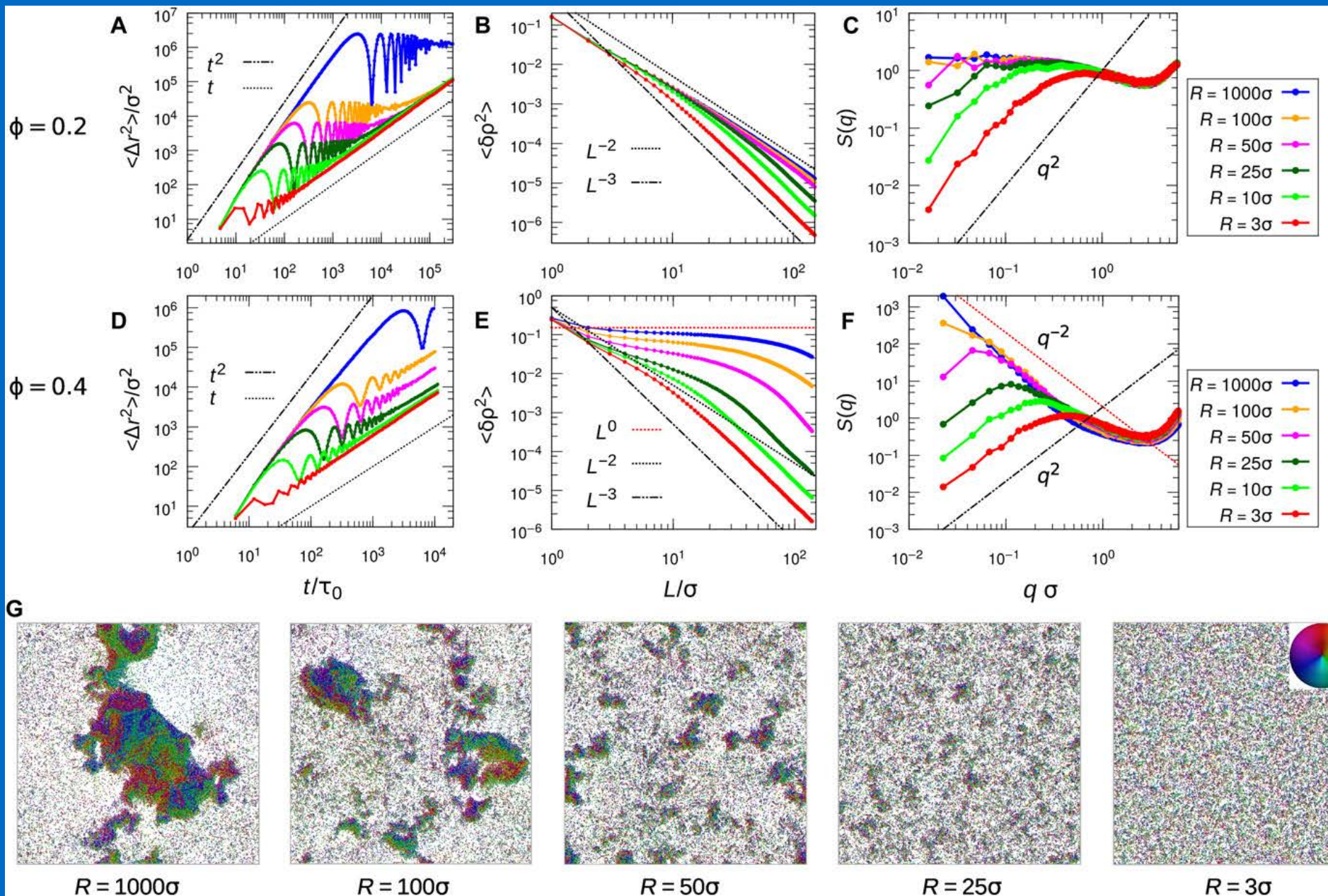
### 3) Hyperuniformity in active systems



Q. L. Lei, M. P. Ciamarra, R. Ni, *Nonequilibrium strongly hyperuniform fluids of circle active particles with large local density fluctuations*, Science Advances **5**, eaau7423 (2019).



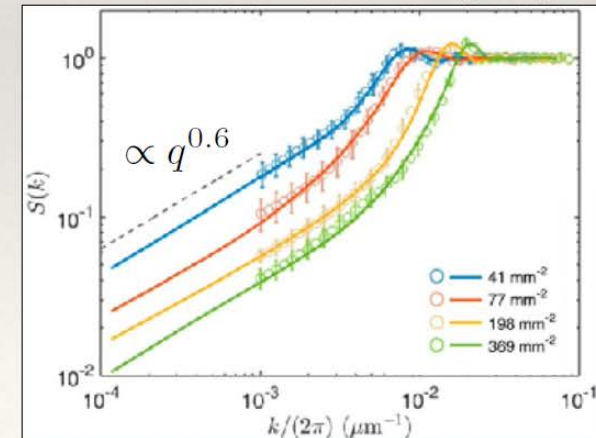
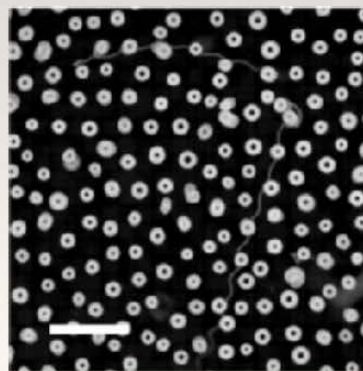
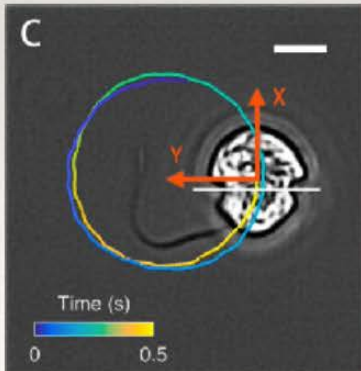
**Fig. 1. Absorbing-active transition.** (A) Schematic of the 2D system of circle active particles. (B) Dynamic phase diagram in the representation of packing fraction  $\phi$  and circle radius  $R$ . (C and D) Typical snapshots of the active and adsorbing states near the critical point with  $\phi = 0.20$  with  $R = 1.75\sigma$ , where the color indicates the self-propulsion orientation of each particle. These two states are marked as magenta and cyan solid symbols, respectively, in (E). (E) MSD as functions of time for system with  $R = 1.75\sigma$  started from random configurations. Red line, active state ( $\phi = 0.22$ ); blue line, absorbing state ( $\phi = 0.01$ ); green line, system near the critical point ( $\phi = 0.20$ ) in which the system ultimately falls into the absorbing state after a long simulation time. (F and G) Diffusion constant as functions of  $\phi$  near the critical point  $\phi_c$  for systems with different  $R$ . The dashed lines are the fitting of power law  $(\phi - \phi_c)^\beta$ . (H and I) The structure factor  $S(q)$  and the orientation correlation function  $C(r)$  of active (magenta) and absorbing (cyan) states as marked by solid symbols in (E). (J) The measured critical exponent  $\beta$  from (G) as a function of  $R$ . For all the calculations,  $N = 10,000$  and  $T_R = 0$ .



from phase separation to hyperuniformity !?

## Experiment example: Algae system

M. Huang *et al.*, (2021)



M. Huang, W. Hu, S. Yang, Q. X. Liu, H. P. Zhang, *Circular swimming motility and disordered hyperuniform state in an algae system*, PNAS **118**, e2100493118 (2021).

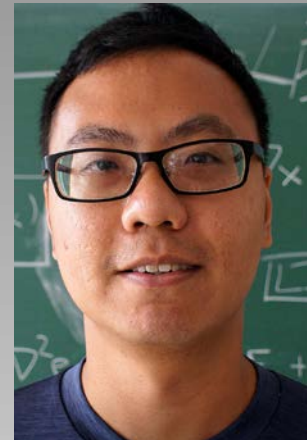
Coarse-grained **theory** by Y. Kuroda, H. Matsuyama, T. Kawasaki, and K. Miyazaki (Nagoya)

using fluctuating hydrodynamic equations (unpublished)

# hyperuniformity in other active systems



Michael A. Klatt



Yuanjian Zheng

Hyperuniformity in phase-separating systems described by generalized (active) Cahn-Hilliard models

## 4) Conclusions

Why does hyperuniformity favorably occur in active systems??

Acknowledgement: R. Wittmann, M. A. Klatt, Y. Zheng, V. A. Debets, L. M. C. Janssen, C. Bechinger, I. Buttinoni, G. Volpe